# 铬青铜与双相不锈钢偏钢电子束焊接头组织及相构成

张秉刚, 何景山, 吴 林, 冯吉才
(哈尔滨工业大学 现代焊接生产技术国家重点实验室, 哈尔滨 150001)

摘 要: 对 QCr0.8与 1Cr21Ni5Ti异种材料对接接头进行了钢侧偏束电子束焊接试验。采用光学金相、电子探针、能谱分析和 X射线衍射相分析方法对接头组织结构、成分分布及相组成进行了研究。研究结果表明, 偏钢焊缝组织大部分为 α+ε支晶相, 且 α相的含量要高于 ε相, 只在焊缝顶部偏铜侧形成了少量的 Cu(ss Fe)相组织, 无脆性相生成; 偏钢量 $h_s$直接影响接头区的组织结构和熔接状况, $h_s$较小时有少量的 QCr0.8金属熔入到焊缝中, 焊缝与 QCr0.8基体的组织和成分差异较大; 随 $h_s$的增加, 虽接头组织均匀化程度有所提高, 但由于不均衡热输入及铬青铜的快速热传导性, 导致铜侧母材的熔合状况不良。$h_s$的小范围增加即可导致 QCr0.8母材的基本不熔化, 形成局部焊合或未焊合的接头。

关键词: 电子束焊接; 组织; 相构成
中图分类号: TG401 文献标识码: A 文章编号: 0253-360X(2005)11-89-04

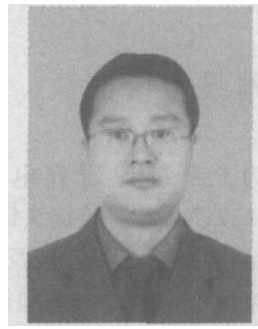

张秉刚

## 0 序 言

QCr0.8作为一种含 Cr量较高的青铜合金, 不仅有着较好的耐蚀性和较高的热导率, 而且具有良好的综合力学性能[1,2], 目前已在国外一些主流发动机的制造中得到普及应用。而双相不锈钢 1Cr21Ni5Ti除了其优异的力学性能及耐全腐蚀性能外, 还具有良好的抗应力腐蚀能力[3,4]。因此, 铬青铜与双相不锈钢异种材料间的有效组合可同时满足发动机推力室的冷却及高强要求, 使其异种材料连接组件在新一代发动机制造中具有广阔的应用前景。作者以加热速度快、焊接热影响区及变形小、适于焊接异种金属的高能电子束作为焊接热源[5,6], 对 QCr0.8与 1Cr21Ni5Ti进行了偏钢电子束焊接试验。研究了电子束偏移作用于钢一侧时, 焊缝中钢母材熔合比增加时的组织和成分分布特征, 揭示了其接头的基本相组成, 为实现 QCr0.8/1Cr21Ni5Ti的可靠高质电子束焊接提供理论和试验基础。

## 1 试验材料及方法

试验用铬青铜及双相不锈钢的化学成分及力学性能见表 1及表 2。

试验用焊接设备为法国 TECHMETA公司生产的 MEDARD45型真空电子束焊机, 焊机最大加速电压 60 kV, 最大功率 6 kW, 试验所使用的阴极直径为 φ2.0mm。铬青铜与双相不锈钢的试件尺寸为 100mm×45mm×2mm, 将清理好的铬青铜与双相不锈钢试件底面平齐沿长边对接放入焊机真空室工作台上的自制夹具中紧贴压靠, 注意使其对接缝间隙最大不得超过 0.25mm。然后在真空度为 5.4×$10^{-2}$ Pa, 加速电压 60 kV、电子束束流 45 mA、焊接速度 1 m/min, 表面聚焦状态下, 改变电子束束斑作

表 1 QCr0.8与 1Cr21Ni5Ti化学成分(质量分数, %)
Table 1 Chemical compositions of QCr0.8 and 1Cr21Ni5Ti

| 材 料 | C | Cr | Fe | Ni | Zn | Si | Mg | Pb | S | P | Ti | Mn | 杂质 |
|---|---|---|---|---|---|---|---|---|---|---|---|---|---|
| QCr0.8 | - | 0.4~0.7 | ≤0.05 | ≤0.03 | ≤0.015 | ≤0.002 | ≤0.002 | ≤0.005 | - | - | - | - | ≤0.80 |
| 1Cr21Ni5Ti | 0.09~0.14 | 20~22 | - | 4.80~5.80 | - | 0.80 | - | - | 0.030 | 0.035 | 5×(C-0.02)~0.80 | 0.80 | - |

收稿日期: 2005-09-12

表 2 QCr0.8与 1Cr21Ni5Ti的力学性能

Table 2 Mechanical properties of QCr0.8 and 1Cr21Ni5Ti

| 材料 | 极限强度 $\sigma_b$ MPa | 屈服强度 $\sigma_{0.2}$ MPa | 延伸率 $\delta_5$(%) |
|---|---|---|---|
| QCr0.8 | 360 | – | ≥25 |
| 1Cr21Ni5Ti | 600 | 350 | 20 |

用于双相钢侧距对接面的束偏值进行施焊，并对焊后试件接头进行微观组织、成分及相组成分析。

## 2 结果与讨论

为了系统地研究电子束偏移作用于 QCr0.8/1Cr21Ni5Ti对接接头钢侧所形成的熔接接头的组织结构特点、成分分布及相组成，进行了电子束偏钢焊接试验。为了分析和讨论的方便，将电子束偏移作用于 QCr0.8/1Cr21Ni5Ti对接接头钢侧的电子束偏束熔接简称为偏钢电子束焊接，将电子束作用于钢侧的束偏量简称为偏钢量，以符号 $h_s$来表示。其焊接接头形式见图 1。

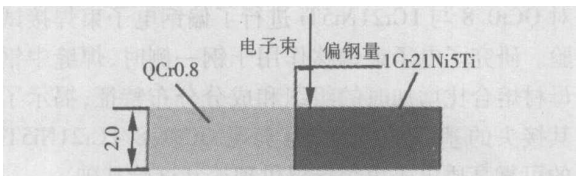


图 1 QCr0.8/1Cr21Ni5Ti厚偏钢电子束焊接接头示意图

Fig. 1 Scheme of equal thickness QCr0.8/1Cr21Ni5Ti EBW Joint with focus on steel side

### 2.1 接头组织形态

图 2是 QCr0.8/1Cr21Ni5Ti偏钢电子束焊接接头的典型组织形貌。可以看出，除在焊缝顶部的偏铜侧有少量间隔分布的细条状灰白色组织外，其整个焊缝基本上是较均匀分布的灰黑色组织，接头的组织形态及分布较均匀。图 3为不同偏钢量 QCr0.8/1Cr21Ni5Ti电子束焊接接头熔合线处组织形貌。由图 3a, b可见，偏钢量为 0.3mm时焊缝组织形态与铬青铜母材相比有明显差异，呈铸态支晶状。此时，铜侧熔合线为一不规则弯曲的曲线，说明部分铬青铜母材已熔化参与焊接成缝，而钢侧熔合线处形成了焊缝与钢侧基体的铸态交错组织。进一步观察发现，在接头铜侧未见有明显的热影响区，在钢侧可见呈较粗大等轴晶的热影响区出现。这是由于电子束偏移作用于钢侧导致钢侧热输入增加，同时双相不锈钢具有比铬青铜更低的热导率，从而使钢侧的热作用程度增大，在钢侧熔合线附近出现了发生再结晶的热影响区，而铜侧热输入的减少及快速的热量散失使其热影响区的范围很窄。

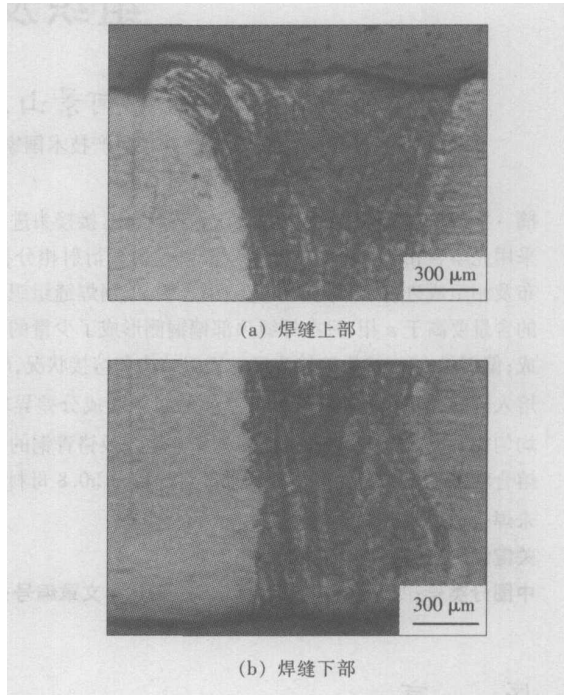


图 2 等厚偏钢焊接头典型组织结构

Fig. 2 Typical microstrostructure of joint with focus on steel side

注：$v$=1m/min, $I_b$=45mA, 表面聚焦, 偏钢量 0.3mm

随着偏钢量的增加，电子束对钢侧的热作用范围及程度逐渐加大，熔池形成过程中钢基体的熔化量也逐渐增加，此时贡献于熔池形成的铬青铜的熔化量相应地逐渐减少。研究发现，在偏钢量为 0.5mm时的接头组织形态分布更趋均匀化，同偏钢量为 0.3mm时的接头相比在焊缝顶部偏铜侧出现的细条状灰白色组织的数量明显减少。进一步增大偏钢量，见图 3c, d此时，可见明显的焊前对接面，接头并未焊合，呈虚焊状。这是由于电子束偏钢量过大，传导到接头对接面铜侧的热量已不足以使其熔化参与有效熔接。这时的焊缝组织为双相不锈钢熔化结晶后的铸态组织，无 Cu元素存在。

### 2.2 接头成分及相构成

为了进一步明确焊缝及热影响区的具体组成成分及元素分布，进行了接头的电子探针扫描及能谱分析。图 4是 $v$=1m/min, $I_b$=45mA、表面聚焦、偏钢量为 0.3mm的接头两侧熔合线附近元素电子探针线扫描结果。由图 4a可以看出，从不锈钢侧母材到焊缝 Fe, Cr, Ni的元素分布曲线并没有大的起伏，

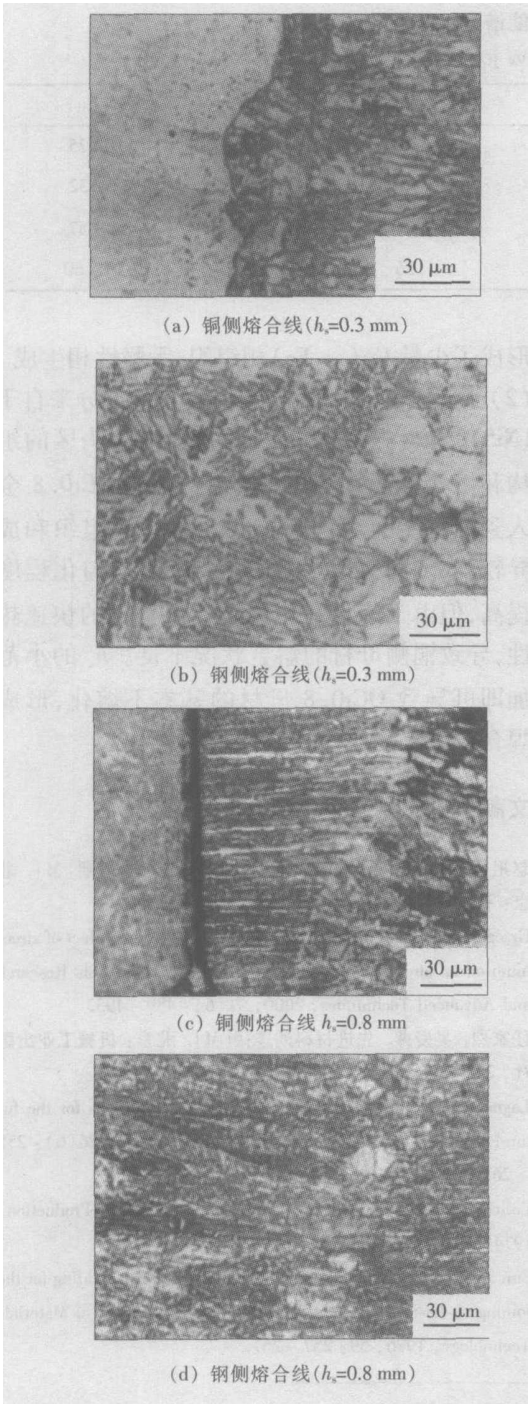


(a) 铜侧熔合线($h_s$=0.3 mm)

(b) 钢侧熔合线($h_s$=0.3 mm)

(c) 铜侧熔合线 $h_s$=0.8 mm

(d) 钢侧熔合线($h_s$=0.8 mm)

图 3　不同偏钢量接头熔合线处组织

Fig. 3　Microstructure near fusion line of the EBW joint with different $h_s$

注：$v$=1 m/min，$I_b$=45 mA，表面聚焦

而是比较平直，说明这三种元素在 1Cr21Ni5Ti中和焊缝中的含量相差很小，Cu元素曲线在焊缝中陡升，即焊缝中熔入了一定量的 Cu元素。由图 4b可以明显看出，焊缝中各主要元素的含量比，其中 Fe、Cr、Ni元素在焊缝中的含量明显高于 Cu元素的含量。由各主要元素在两侧熔合线附近的分布曲线可以看出，焊缝中 Fe、Cr、Ni、Cu元素的分布比较均匀，整个焊缝及两侧热影响区元素分布曲线未有小平台出现，说明没有金属间化合物生成。

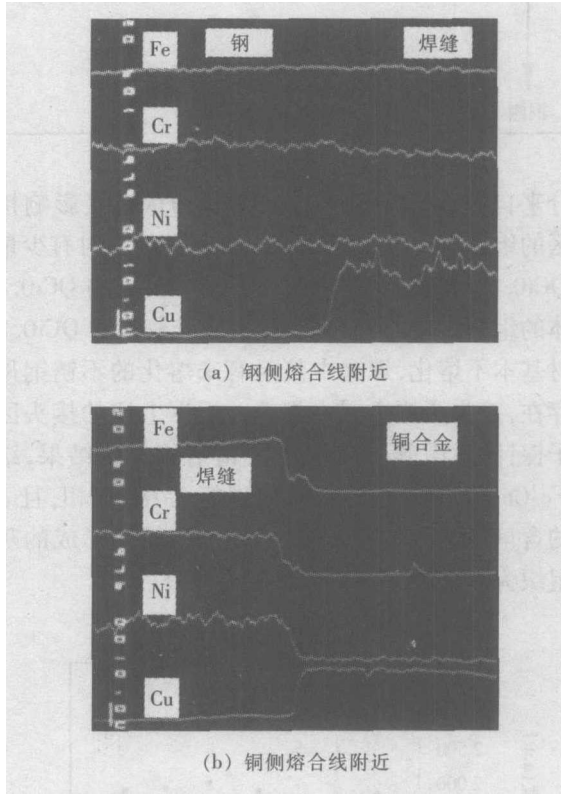


图 4　等厚偏钢电子束焊接头元素分布

Fig. 4　EPMA result of EBW joint with focus on steel side

注：$v$=1 m/min，$I_b$=45 mA，表面聚焦，$h_s$=0.3 mm

表 3为 $v$=1 m/min，$I_b$=45 mA，表面聚焦，$h_s$=0.3 mm的接头区能谱分析结果。可以看出，焊缝区金属的化学成分比较均匀，焊缝组织中 Fe、Cr的含量比较高，Cu已熔入并扩散到整个焊缝及钢侧熔合线处，但含量较少。对焊缝上部偏铜侧的灰白色组织也进行了能谱分析，结果发现该区域 Cu的含量比较高，摩尔分数达到 70.82%，而 Fe只占 20.54%，说明该区域的焊缝金属组织主要来自于铬青铜母材熔化的贡献。

由上述的接头区电子探针元素分布及能谱分析可知，焊缝金属中主要以钢侧母材中的主元素含量为主。这主要是由于电子束偏移作用于钢侧，导致双相不锈钢母材在焊接过程中熔化量增大的缘故。为了进一步确定焊缝中的具体相组成，进行了接头区的 X射线衍射相分析，其分析结果见图 5。由图 5可见，焊缝组织主要以 Fe、Cu相为主，无金属间化合物生成，Cr、Ni相的出现说明偏钢焊时双相钢基体金属的熔化量明显增大。

综上所述，等厚偏钢电子束焊缝中金属元素大

表 3 QCr0.8/1Cr21Ni5Ti电子束偏钢焊接头能谱分析结果(摩尔分数,%)

Table 3 EDX result of QCr0.8/1Cr21Ni5Ti EQW joint with focus on steel side

| 钢侧 | 测试部位 | 测试面域序号 | Fe | Cr | Ni | Cu |
|---|---|---|---|---|---|---|
| | 钢基体 | 1 | 71.51 | 21.77 | 6.45 | 0.25 |
| | 焊缝区 | 2 | 65.93 | 21.63 | 4.10 | 8.32 |
| ↓ | | 3 | 65.86 | 22.04 | 4.50 | 7.57 |
| 铜侧 | 铜基体 | 4 | 0.13 | 1.26 | 0.00 | 98.60 |

部分来自于 1Cr21Ni5Ti母材。偏钢量直接影响接头区的组织结构和熔接状况。偏钢量较小时有少量的 QCr0.8元素熔入并扩散到焊缝中,焊缝与 QCr0.8基体的组织和成分差异较大;偏钢量较大时 QCr0.8母材基本不熔化,焊缝中甚至有未熔化的不锈钢母材存在,接头两侧金属未焊合。根据上述的接头区电子探针、能谱分析及 X射线衍射相分析结果,结合 Fe-Cu相图,推断偏钢焊缝组织为 α+ε相,且 α相的含量要高于 ε相;在焊缝顶部偏铜侧形成的灰白组织为以 Cu(ss Fe)相为主的组织。

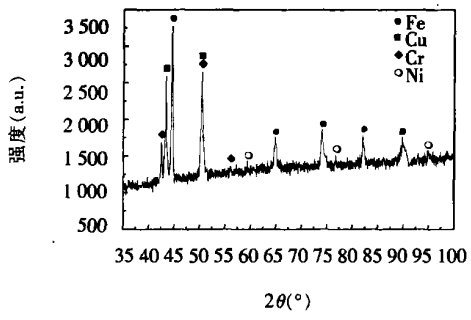


图 5 典型偏钢电子束焊接接头 X射线衍射相分析结果

Fig. 5 Typical XRD result of EBW joint with focus on steel side

## 3 结 论

(1) QCr0.8/1Cr21Ni5Ti偏钢电子束焊接接头组织宏观分布较均匀。焊缝组织大部分为 α+ε支晶相,且α相的含量要高于 ε相,只在焊缝顶部偏铜侧形成了少量 Cu(ss Fe)相组织,无脆性相生成。

(2) 偏钢电子束焊缝中金属元素大部分来自于 1Cr21Ni5Ti母材。偏钢量 $h_s$ 直接影响接头区的组织结构和熔接状况,$h_s$ 较小时有少量的 QCr0.8金属熔入到焊缝中,焊缝与 QCr0.8基体的组织和成分差异较大;随 $h_s$ 的增加,虽接头组织均匀化程度有所提高,但由于不均衡热输入及铬青铜的快速热传导性,导致铜侧母材的熔合状况不良。$h_s$ 的小范围增加即可导致 QCr0.8母材的基本不熔化,形成局部焊合或未焊合的接头。

参考文献:

[1] 赵祖德,姚良均,郭鸿运,等. 铜及铜合金材料手册[M]. 北京:科学出版社, 1993. 25-28.

[2] Grzegorzewicz T, Kuznicka B, Krajczyk. Modifying effect of zirconium on an aluminum-chromium bronze[J]. Materials Research and Advanced Techniques, 2000, 91(6): 489-493.

[3] 任家烈,吴爱萍. 先进材料的连接[M]. 北京:机械工业出版社, 2000. 56-61.

[4] Lagneborg R. Steel development review and prospects for the future[J]. Scandinavian Journal of Metallurgy, 1997, 26(6): 255-265.

[5] College R R. Electron beam welding[J]. Tooling & Production, 1974, (6): 66-67.

[6] Sun Z, Karppi R. The application of electron beam welding for the joining of dissimilar metals: an overview[J]. Journal of Materials Technology, 1996, 59: 257-267.

作者简介:张秉刚,男,1971年 9月出生,工学博士,讲师。主要研究方向为新材料及异种材料电子束焊接,发表论文 10余篇。

Email: zhanghg@hit.edu.cn

was low, changing rotation speed did not change tensile strength; with high welding speed, higher rotation speed was bad for tensile strength. When welding speed and rotation speed were both low, the mechanical properties of joints welded with non-threaded tool are better than those with threaded tool; increasing welding speed and rotation speed did not influence tensile strength.

**Key words**: FSW; aluminum; process parameter; mechanical properties of the joint

**Spatial distribution features of weld defects in complex structure**

SHI Duan-hu, GANG Tie, YUAN Yuan(State Key Lab of Advanced Welding Production Technology, Harbin Institute of Technology, Harbin 150001, China). p71 - 74

**Abstract**: X-ray real time imaging method was adopted to nondestructively test the complex structure welding parts of titanium alloys, the spatial position of tiny flaws was determined based on the line profile distribution of flaws position, and a formula which could calculate the burial depth of flaws was obtained. According to the characteristic of abnormal peak and abnormal slant-concave flaw, an automatic extraction algorithm of projection distance was presented individually. Experimental results showed that the above algorithm can figure out the projection distance very well and can determine the spatial distribution features of the flaws.

**Key words**: titanium alloy laser welding; ray detection; tiny flaw; line profile; spatial distribution features

**Simulation of the influence of scan path on temperature field in the welding rapid prototyping** HU Rong-hua, ZHANG Hua, XU Jianning, WAN Ling-na(Mechanical and Electronic School, Nanchang University, Nanchang 330029, China). p75 - 78

**Abstract**: The part fabricated by welding rapid prototyping has excellent mechanics capability, so welding prototyping will be widely applied in the future. But welding is a processing of local high temperature, the distribution of temperature field will affect the quality and performance of welding part. In this paper, one-layer depositing of thin-wall part was studied. Numerical simulation was done by ANSYS, and the influences of scan path on temperature field and stress field were analyzed. This study will offer theoretical foundation to accurataly choose the scan path in the welding rapid prototyping.

**Key words**: rapid prototyping based welding; scan path; temperature field; simulation

***Distribution and control of residual stresses in FSW joints*** CHAI Peng, LUAN Guo-hong, GUO De-lun, LI Ju(Beijing Aeronautical Manufacturing Technology Research Institute, Beijing 100024, China). p79 - 82

**Abstract**: Deformation of FSW stractures welded with different parameters and tools was measured and analyzed in this paper. Results showed that smaller tool shoulder and lower welding energy would reduce the deformation. With optimized welding parameters, dynamic control of welding deformation(DC-LSND) which was usually used in TIG was introduced to FSW, and its effects on structure deformation and residual stresse were also studied.

**Key words**: friction stir welding, residual stress, dynamic control low stress no distortion

**Preliminary study on friction stir welding of titanium alloy**

LUAN Guo-hong, CHAI Peng, SUN Chengbin(P. O. Box 340, China FSW Center, Beijing 100024, China). p83 - 88

**Abstract**: According to the analysis of the thermophysical characteristics of several conventional titarcium alloys, friction stir weldability of titanium alloy had been discussed in this paper. According to the features of Ti alloy, the pin tool, welding anvil and protecting device were designed and applied for the friction stir welding of Ti alloy. By observation of the weld appearances and microstructures of the joint, as well as the mechanical property testing, the results showed that Ti-6Al-4V alloy can be successfully welded by FSW, and tensile strength of the joint can reach up to 90% of the base metal. With optimization of the welding parameter, procedure, pin tool profile and material, the property and performance of FSW of Ti alloy shall be unproved.

**Key words**: friction stir welding; titanium alloy; weldability

**Microstructures and phase composition of QCr0. 8/1Cr21Ni5Ti joint by EBW with focus on sdteel side** ZHANG Bing-gang, HE Jing-shan, WU Lin, FENG Ji-cai(State Key Laboratory of Advanced Welding Production Technology, Harbin Institute of Technology, Harbin 150001, China). p89 - 92

**Abstract**: Electron beam welding experiments of QCr0. 8/1Cr21Ni5Ti dissimilar butt joint were carried out. The microstructures, elements distribution and phase composition of the joint were investigated by means of Optical Micrography, EPMA, EDX and XRD. The results showed that the microstructure of joint mostly consists of phase $\alpha + \varepsilon$, and phase $\alpha$ was quantitatively more than phase $\varepsilon$. A few of Cu(ss. Fe) phase formed only in top weld near to copper side and any brittle phase was not generated in the whole weld. The microstructures and bonding

status of joint were evidently affected by changing of $h_s$ (i. e. beam offset on steel side), a small quantity of metal QCr0. 8 melted down into weld as value of $h_s$ was less, a large difference of microstructures and chemical composition existed in comparison of weld with base metal QCr0. 8. With increasing of $h_s$ the microstructure distribution of joint becomes homogeneous gradually, but the bad fusion's status happened to QCr0. 8 side in weld due to unbalanced heat input and rapid heat conduction of QCr0. 8. Even if $h_s$ increased in little range, base metal QCr0. 8 may not be fusion, which resulted in forming joint of local fusion or lack of fusion.

**Key words**: electron beam welding; microstructure; phase composition

**Hydrogen behavior in titanium alloy EBW joints** WANG Ya-jun[1,2], TANG Xiao-qing[1], LIU Hao[2], GUAN Qiao[2] (1. Beijing hangkong university, Beijing 100083, China; 2. Beijing aeronautical manufacture technology research institute. Beijing 100024, China). p93 - 96

**Abstract**: The electrolytic hydrogen charging with constant current and X - ray diffraction were used to investigate the hydrogen content threshold of the hydrogen induced cracking for Ti1023 titanium alloy EBM joints and the effect of the microstructure phase on sensitivity of hydrogen induced cracking. The scanning electronic microscopy was employed to observe the fracture appearance on different hydrogen charging condition. By means of the artificial aging and ion probe analysis, the dynamic behavior of hydrogen in Ti1023 titanium alloy EBM joints was also studied in this paper.

**Key words**: Ti1023 titanium alloy; EBM; hydrogen induced cracking

**Application of fuzzy-PID control on seam tracking for welding-robot** YE Jian-xiong, ZHANG Hua (school of Mechanical and Electronic Engineering, Nanchang University, Nanchang 330029, China). p97 - 100

**Abstract**: A convenient and effective close loop control scheme, had been proposed to satisfy the aim of seam tracking based on the analysis of the welding-robot modeling and its control link in this paper. With the introduction of fuzzy controller and PID controller and with the adoption of the simulation on the differentiated modeling, the characteristics of the hybrid manipulator were illuminated. In the end, some conclusions were drawn on the base of analysis of the different response curves.

**Key words**: fuzzy; PID; hybrid-manipulator; self-adaptation; simulation

**Ultrasonic signal analyses of spot welds in thin steel sheet** ZHAO Xin-yu, GANG Tie, YUAN Yuan (State key Laboratory of Advanced Welding Production Technology, Harbin Institute of Technology, Harbin 150001, China). p101 - 105

**Abstract**: The quality of spot welds in galvanized sheet metal was evaluated by using ultrasonic water immersion focusing method. The A-scan signal, B- and C-scan image features of spot welds were analyzed. The feasibility of evaluating the quality of spot welds by using the B-scan image was provided. By using the method, not only the kiss bonding and the perfect joint could be evaluated qualitatively, but also the pressure mark depth of the upper-bottom surface and the spot weld diameter could be calculated quantitatively. The accuracy of testing result was verified by contrasting the metallographs of actual spot welds cross section.

**Key words**: ultrasonic test; water immersion focusing; resistance spot weld

**Comparison of fatigue property for TIG welding of TC4 and TA15 tianium alloy** WANG Xiang-ming (Shenyang Aircraft Design & Research Institute, Shenyang 110035, China). p106 - 108

**Abstract**: As the researched objects, TIG welded test specimens of titanium TC4 and TA15 were selected, and their fatigue tests were done under different constant amplitude spectrums with four stress levels, respectively. According to the contrast analysis for the fatigue test results by use of three-parameter-model of fatigue life founded in this paper, the fatigue property of TA15 TIG weld was better than TC4 TIG weld appreciably in $10^4 \sim 10^6$ region. The possible affected factors were discussed.

**Key words**: Titanium; weld; fatigue

**Experimeneal research on high Temperature CTOD of electron beam welded joints of GH4169 alloy** WU Bing[1], ZUO Cong-jin[1], LI Jin-wei[1], ZHANG Yan-hua[2], XIONG Lin-yu[2] (1. BAMTRI, Key laboratory for high energy density beam processing technology, Beijing 100024, China; 2. Beijing University of Aeronautics and Astronautics, Beijing 100083, China). p109 - 112

**Abstract**: In accordance with GB/T 2358-94, CTOD (crack-tip opening diaplacement) tests were conducted at 650 ℃ for electron beam welded joints of GH4169 alloy. According to the requirements of the standard, the specimen was a standard SE(B) (three point bending), the results were calculated using the P-V curves of parent material and weld metal. Finally, the test results were summarized and analysed.

**Key words**: electron beam welding; GH4169; high temperature; CTOD